Research Article

For reprint orders, please contact: reprints@future-science.com

Future Medicinal Chemistry

Second generation 4,5,6,7-tetrahydrobenzo[*d*]thiazoles as novel DNA gyrase inhibitors

Andraž Lamut[1], Žiga Skok[1], Michaela Barančoková[1], Lucas J Gutierrez[2], Cristina D Cruz[3], Päivi Tammela[3], Gábor Draskovits[4], Petra Éva Szili[4,5], Ákos Nyerges[4], Csaba Pál[4], Peter Molek[1], Tomaž Bratkovič[1], Janez Ilaš[1], Nace Zidar[1], Anamarija Zega[1], Ricardo D Enriz[2], Danijel Kikelj[1] & Tihomir Tomašič*,[1]

[1]Faculty of Pharmacy, University of Ljubljana, Aškerčeva cesta 7, Ljubljana, 1000, Slovenia

[2]Facultad de Química, Bioquímica y Farmacia, Universidad Nacional de San Luis, IMIBIO-CONICET Chacabuco 915, San Luis, 5700, Argentina

[3]Drug Research Programme, Division of Pharmaceutical Biosciences, Faculty of Pharmacy, University of Helsinki, P.O. Box 56 (Viikinkaari 5 E), Helsinki, FI-00014, Finland

[4]Synthetic & Systems Biology Unit, Institute of Biochemistry, Biological Research Centre of the Hungarian Academy of Sciences, Szeged, H-6726, Hungary

[5]DoctoralSchool of Multidisciplinary Medical Sciences, University of Szeged, Szeged, H-6726, Hungary

*Author for correspondence: Tel.: +386 1 476 9556; tihomir.tomasic@ffa.uni-lj.si

Aim: DNA gyrase and topoisomerase IV are essential bacterial enzymes, and in the fight against bacterial resistance, they are important targets for the development of novel antibacterial drugs. **Results:** Building from our first generation of 4,5,6,7-tetrahydrobenzo[*d*]thiazole-based DNA gyrase inhibitors, we designed and prepared an optimized series of analogs that show improved inhibition of DNA gyrase and topoisomerase IV from *Staphylococcus aureus* and *Escherichia coli*, with IC_{50} values in the nanomolar range. Importantly, these inhibitors also show improved antibacterial activity against Gram-positive strains. **Conclusion:** The most promising inhibitor, **29**, is active against *Enterococcus faecalis*, *Enterococcus faecium* and *S. aureus* wild-type and resistant strains, with minimum inhibitory concentrations between 4 and 8 μg/ml, which represents good starting point for development of novel antibacterials.

Graphical abstract:

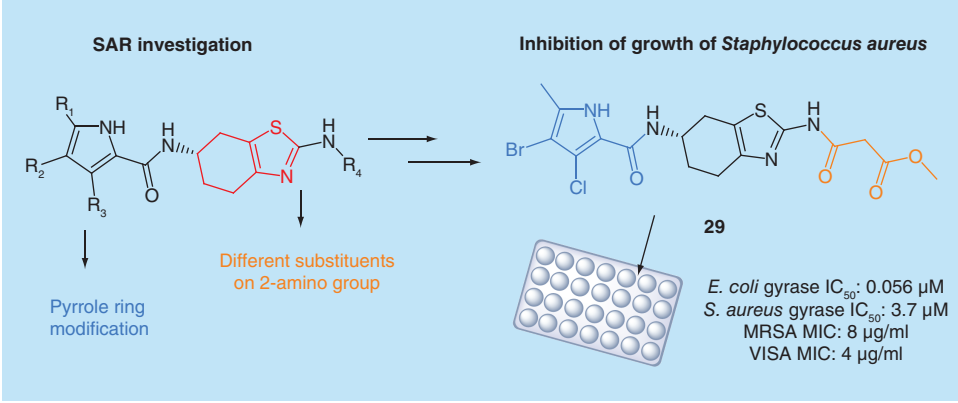

First draft submitted: 18 April 2019; Accepted for publication: 23 October 2019; Published online: 11 February 2020

Keywords: antibacterial • DNA gyrase • inhibitor • pyrrolamide • QTAIM • thiazole

Many clinically important pathogenic microorganisms have become resistant to the currently available antibiotics. In 2017, the WHO published a list of priority pathogens for which new antibiotic treatments are urgently

newlands press

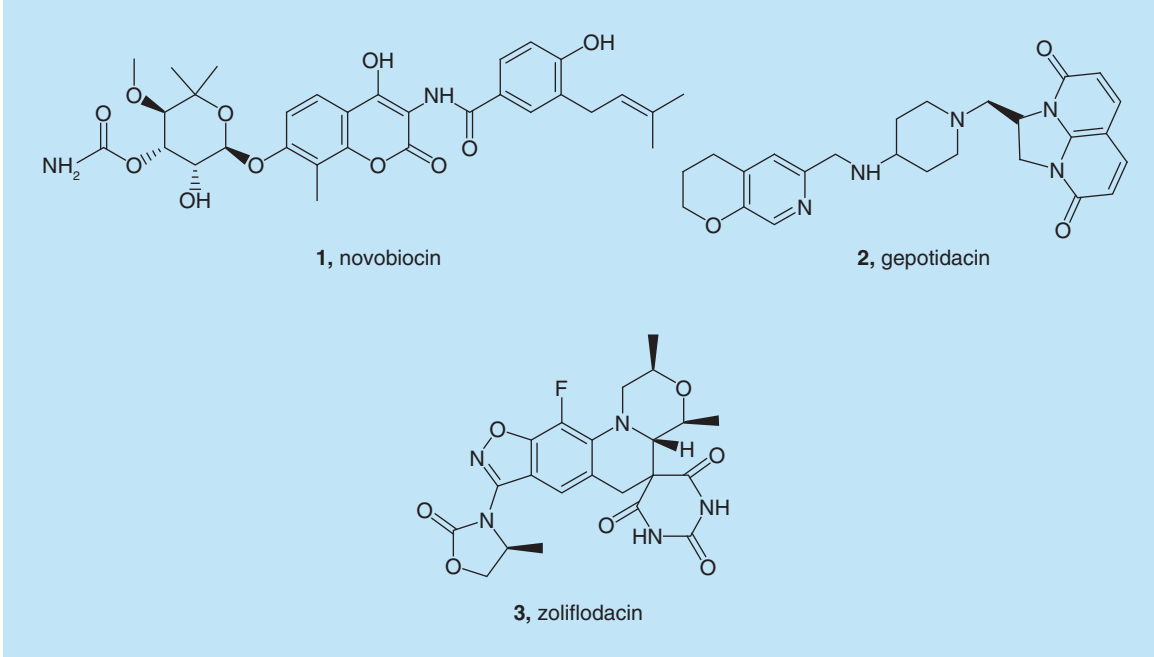

Figure 1. DNA gyrase inhibitor novobiocin, and two novel DNA gyrase and topoisomerase IV inhibitors in clinical development.

needed [1,2]. The reasons for this development of multidrug-resistant microorganisms include inappropriate prescribing and consuming of antibiotics, false dose regimens and extensive agricultural use of antimicrobials. The available treatment options for infections caused by multidrug-resistant bacteria have also worsened because of a substantial reduction in newly approved antibacterials over the past two decades [3]. Fortunately, clinicians have recognized bacterial resistance as one of the major human health threats, and antibacterial drug discovery that targets the multidrug-resistant strains has recently gained more research interest. To overcome the issue of antibiotic resistance, there is the need for the development of antibacterial agents with new mechanisms of action [4] and with multitargeting drugs that simultaneously inhibit different bacterial targets, for which the bacterial development of target-based resistance will be slower [5].

Bacterial topoisomerases have important roles in replication of DNA through their catalysis of modifications to its topological state during replication [6,7]. Topoisomerase inhibition leads to complete loss of cell viability and bacterial cell death [7,8]. DNA gyrase and topoisomerase IV are type IIA topoisomerases that show high structural and sequence similarity and are composed of two subunits, GyrA and ParC, respectively, and GyrB and ParE, which contain the ATPase active site [9]. These two enzymes are validated and attractive targets for antibacterial drug discovery [10,11]. The catalytic GyrA and ParC subunits are inhibited by the therapeutically used fluoroquinolone class of antibiotics [12,13]. Moreover, inhibition of the ATP-binding GyrB and ParE subunits is also a promising strategy for the development of new antibacterial drugs [9,10,14]. For example, the aminocoumarin antibiotic novobiocin (**1**; Figure 1) was previously used in therapy, although it was withdrawn because of resistance development and the discovery of safer and more effective antibacterial drugs [10]. Furthermore, novel DNA gyrase and topoisomerase IV inhibitors that belong to different chemical classes with distinct modes of action are now in clinical development (e.g., gepotidacin, **2** [15]; zoliflodacin, **3** [16]; Figure 1) [11]. The structural similarities between DNA gyrase and topoisomerase IV offer the opportunity to design dual-targeting inhibitors for which the bacterial target-based resistance will develop more slowly compared with compounds that inhibit a single target. Besides, there is no cross-resistance between inhibitors that bind to the catalytic (e.g., fluoroquinolones) and ATPase (e.g., novobiocin) subunits of DNA gyrase and topoisomerase IV [17].

As the targeting of the ATP-binding site of bacterial DNA gyrase can be associated with selectivity issues in terms of human ATP-binding enzymes, determination of the selectivity toward structurally similar enzymes is of great importance [18]. Selectivity of GyrB and ParE inhibitors against eukaryotic topoisomerase II can be achieved by exploiting the important differences between the amino-acid residues that comprise the inhibitor-binding sites

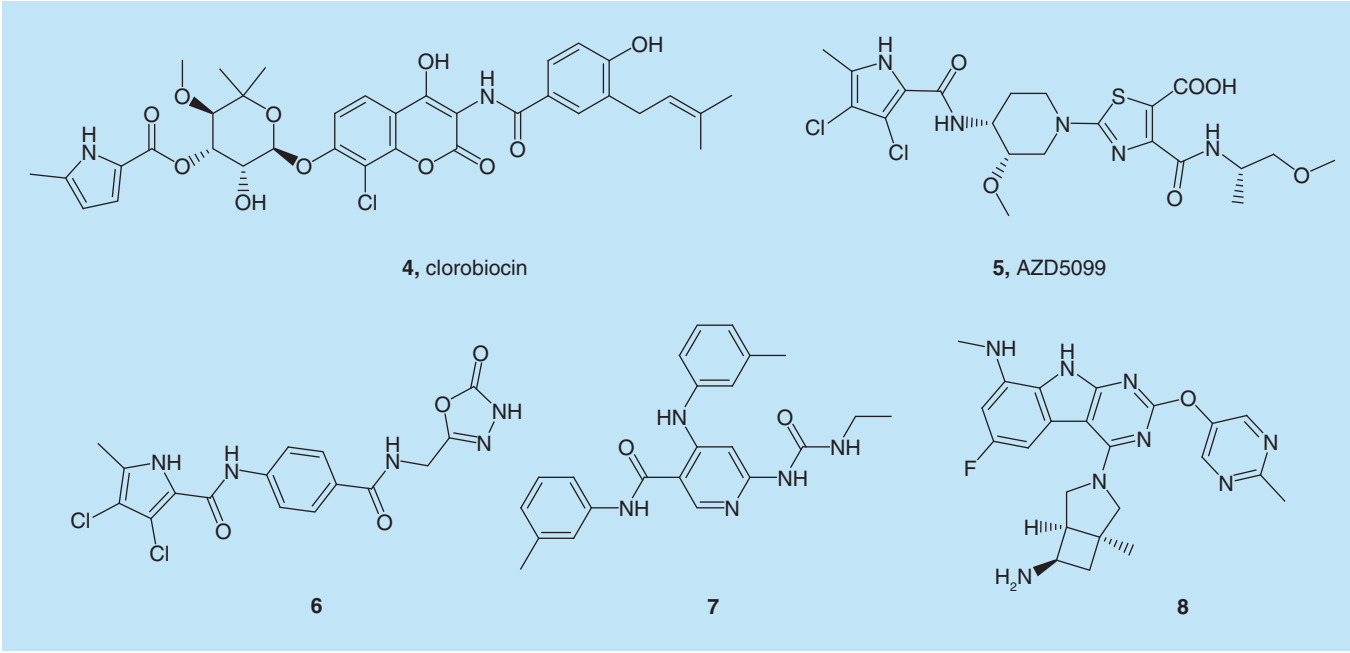

Figure 2. Representative GyrB and ParE inhibitors of natural and synthetic origins.

of the human and bacterial topoisomerases. Moreover, although seldom reported, the selectivity profiles against human protein kinases are usually good [9,18,19]. The potential drawback of targeting the ATP-binding site of DNA gyrase remains toxicity, which was an issue associated with many of the newly discovered DNA gyrase inhibitors in the past [10]. Moreover, ATP-competitive DNA gyrase inhibitors do not increase the concentration of enzyme-DNA cleavage complexes, which is the mechanism characteristic for fluoroquinolone class of DNA gyrase inhibitors [20].

Our first GyrB inhibitors were discovered through virtual screening of a designed library of marine alkaloid analogs, among which the 4,5,6,7-tetrahydrobenzo[*d*]thiazoles were shown to be the most potent [21]. Following our initial discovery and optimization of the virtual screening hits [21], we designed and prepared several series of *N*-phenylpyrrolamides as a new structural class of potent GyrB inhibitors with antibacterial activities [22–25]. In addition, the benzothiazole-2,6-diamine scaffold was introduced in the place of the 4,5,6,7-tetrahydrobenzo[*d*]thiazole, to obtain analogs with low nanomolar inhibition of *Escherichia coli* DNA gyrase and improved inhibition of *E. coli* topoisomerase IV [26]. To further explore the structure–activity relationships (SARs) of the 4,5,6,7-tetrahydrobenzo[*d*]thiazoles, a series of »reversed« analogs and ring-opened inhibitors was also synthesized. However, these compounds showed only (sub)micromolar DNA gyrase inhibition and poor antibacterial activities due to the loss of the important cation–π interactions in the binding site [27]. A common feature of all of these inhibitors is the pyrrole moiety, which is also found in some other structural classes of GyrB inhibitors with antibacterial properties, such as the natural antibiotics clorobiocin (**4**; Figure 2) [28] and kibdelomycin [29], as well as synthetic inhibitors like aminothiazoles (**5**, AZD5099; Figure 2) [30] and *N*-phenylpyrrolamides (**6**; Figure 2) [25]. In addition to the pyrrole-containing compounds, potent GyrB and ParE inhibitors were also identified in other structural classes, such as ethyl ureas, which are mainly active against Gram-positive bacteria [31] (**7**; Figure 2), and tricyclic inhibitors [19] (**8**; Figure 2), which are also active against Gram-negative strains.

Although the first generation of 4,5,6,7-tetrahydrobenzo[*d*]thiazole inhibitors showed potent *E. coli* DNA gyrase inhibition, their activities against *E. coli* topoisomerase IV and *Staphylococcus aureus* DNA gyrase and topoisomerase IV were more than 100-fold weaker. This thus resulted in poor antibacterial activities against the tested Gram-positive bacterial strains. The compounds were also not active against the tested Gram-negative strains, which were mainly attributed to their poor penetration and active efflux from the bacterial cytoplasm [21]. By measuring the volumes of the hydrophobic pockets of *E. coli* and *S. aureus* GyrB and ParE, where the pyrrolamide moiety of inhibitors is bound in the available crystal structures, we noted that the pocket volume in *E. coli* GyrB is larger compared with the other three enzymes. Therefore, poor inhibition of *S. aureus* DNA gyrase and *S. aureus* and *E. coli* topoisomerase IV might be explained by steric clashes of the 4,5-dibromo- and 4,5-dichloro-pyrrolamide

10.4155/fmc-2019-0127

moieties in the hydrophobic pocket. The aim of the present study was thus to further explore the SARs around the 4,5,6,7-tetrahydrobenzo[*d*]thiazole scaffold, to improve the inhibition of DNA gyrase and topoisomerase IV, which would also result in improved antibacterial activities.

Experimental section

Materials & methods

The chemicals were obtained from Acros Organics (Geel, Belgium), Sigma-Aldrich (MO, USA), TCI Europe N.V. (Zwijndrecht, Belgium) and Apollo Scientific (Stockport, UK), and were used without further purification. Analytical TLC was performed on silica gel Merck 60 F_{254} plates (0.25 mm), using visualization with UV light and spray reagents. Column chromatography was carried out on silica gel 60 (particle size, 240–400 mesh). HPLC analyses were performed on: Agilent Technologies 1100 instrument with a UV–Vis detector (G1365B), a thermostat (G1316A), an autosampler (G1313A) and a C18 column (Eclipse Plus; 5 µm, 4.6 × 150 mm; Agilent, CA, USA); Thermo Scientific Dionex Ultimate 3000 Binary Rapid Separation LC System (Thermo Fisher Scientific, MA, USA) with an autosampler, a binary pump system, a photodiode array detector, a thermostated column compartment and a C18 column (Zorbax Extend; 3.5 µm, 4.6 × 150 mm; Agilent, CA, USA). The following gradient elution method was used with mobile phases A (0.1% trifluoroacetic acid in water) and B (acetonitrile): 0–16 min, 95–5% A; 16–21 min, 5% A. The flow rate was 1.0 ml/min, and the injection volume was 20 µl. All of the tested compounds were ≥95% pure by HPLC. Melting points were determined on a Reichert hot-stage microscope, and are uncorrected. ^{1}H and ^{13}C NMR spectra were recorded at 400 and 100 MHz, respectively, on an AVANCE III 400 spectrometer (Bruker Corporation, MA, USA) in DMSO-d_6, $CDCl_3$, or MeOD-d_4 solutions, with tetramethylsilane (TMS) as the internal standard. Mass spectra were obtained using a Q-TOF Premier mass spectrometer (Micromass, Waters, Manchester, UK) or an expression compact mass spectrometer (Advion Inc., NY, USA) or Exactive™ Plus Orbitrap mass spectrometer (Thermo Fischer Scientific Inc., MA, USA). Optical rotations were measured on a polarimeter (241 MC; Perkin-Elmer, MA, USA). The reported values for specific rotation were the means of ten successive measurements, using an integration time of 5 s.

Determination of inhibitory activities against *E. coli* & *S. aureus* DNA gyrase & topoisomerase IV

The assays for the determination of IC_{50} values against *E. coli* and *S. aureus* DNA gyrase and topoisomerase IV were performed according to the previously reported procedures [21].

Determination of inhibitory activities against human DNA topoisomerase II

The inhibitory activities against human DNA topoisomerase II were determined in an assay on streptavidin-coated 96-well microtiter plates (Inspiralis, Norwich, UK, Thermo Scientific Pierce, MA, USA). First, the plates were rehydrated with buffer (20 mM Tris-HCl, 0.01% [w/v] bovine serum albumin (BSA), 0.05% [v/v] Tween 20, 137 mM NaCl, pH 7.6), and then the biotinylated oligonucleotide was immobilized. After washing off the unbound oligonucleotide, the enzyme assay was performed. The reaction volume of 30 µl in buffer (50 mM Tris-HCl, 10 mM $MgCl_2$, 125 mM NaCl, 5 mM dithiothreitol, 0.1 µg/ml albumin, 1 mM ATP, pH 7.5) contained 1.5 U human DNA topoisomerase II, 0.75 µg supercoiled pNO1 plasmid and 3 µl of the inhibitor solution in 10% DMSO containing 0.008% (v/v) Tween 20. The reaction solutions were incubated at 37°C for 30 min. Then, triplex forming (TF) buffer (50 mM NaOAc, 50 mM NaCl, 50 mM $MgCl_2$, pH 5.0) was added to terminate the enzymatic reaction. After an additional incubation for 30 min at room temperature, during which the biotin–oligonucleotide–plasmid triplex was formed, the unbound plasmid was washed off using TF buffer, and Diamond Dye was added in T10 buffer (10 mM Tris-HCl, 1 mM EDTA, pH 8.0). The fluorescence was measured with a microplate reader (BioTek Synergy H4; excitation, 485 nm; emission, 537 nm). The initial screening was at 100 or 10 µM inhibitor. For the most active inhibitors, the IC_{50} values were determined using seven concentrations of the tested compounds. The GraphPad Prism 6 software was used to calculate the IC_{50} values. The results are reported as the mean values of three independent measurements. Etoposide was used as the positive control (IC_{50}: 59 µM).

Determination of antibacterial activities

Clinical microbiology control strains of *Enterococcus faecalis* (ATCC 29212), *S. aureus* (ATCC 25923), *E. coli* (ATCC 25922), *Pseudomonas aeruginosa* (ATCC 27853), *Enterococcus faecium* (ATCC 700221) and vancomycin-intermediate *S. aureus* (ATCC 700699) were obtained from Microbiologics Inc. (MN, USA). Methicillin-resistant *S. aureus* (ATCC 43300) and *S. aureus* (ATCC 29213) strains, which were used for additional testing (Table 6), were

Table 1. Inhibition of *Escherichia coli* and *Staphylococcus aureus* DNA gyrase and topoisomerase IV by the 4,5,6,7-tetrahydrobenzo[*d*]thiazoles 20–41, which contain differently substituted pyrrole moieties (type I compounds).

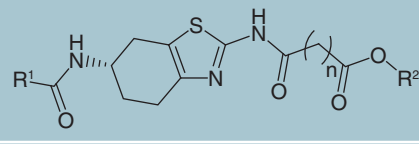

Compound	R^1	R^2	n	DNA gyrase IC_{50} [μM] or RA [%]†		Topoisomerase IV IC_{50} [μM] or RA [%]†	
				Escherichia coli	*Staphylococcus aureus*	*Escherichia coli*	*Staphylococcus aureus*
NB‡	-	-	-	IC_{50}: 0.17	IC_{50}: 0.040	IC_{50}: 11	IC_{50}: 27
20¶	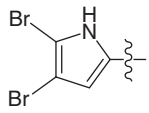	Me	1	IC_{50}: 0.096 ± 0.060	IC_{50}: 110 ± 10	IC_{50}: 86 ± 24	RA: 74
21	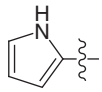	Me	1	RA: 100	n.t.	n.t.	n.t.
22	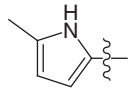	Me	1	RA: 94	n.t.	n.t.	n.t.
23	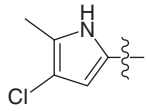	Me	1	IC_{50}: 0.32 ± 0.02	IC_{50}: 8.4 ± 0.7	RA: 61	RA: 95
24	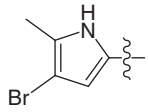	Me	1	IC_{50}: 0.60 ± 0.19	IC_{50}: 31 ± 23	IC_{50}: 230 ± 120	IC_{50}: 35 ± 4
25	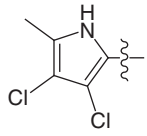	Et	0	IC_{50}: 0.23 ± 0.05	IC_{50}: 0.71 ± 0.32	RA: 91	RA: 96
26	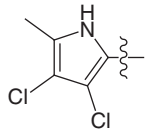	Me	1	IC_{50}: 0.29 ± 0.10	IC_{50}: 26 ± 3	RA: 94	RA: 98
27	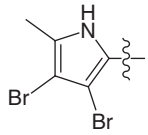	Me	1	IC_{50}: 0.15 ± 0.02	IC_{50}: 31 ± 4	RA: 98	RA: 100

†RA of the enzyme at 10 μM tested compound
‡NB was used as positive control.
¶data published previously [21].
IC_{50}: The half maximal inhibitory concentration; NB: Novobiocin; n.t.: Not tested; RA: Residual activity.

10.4155/fmc-2019-0127

Table 1. Inhibition of *Escherichia coli* and *Staphylococcus aureus* DNA gyrase and topoisomerase IV by the 4,5,6,7-tetrahydrobenzo[*d*]thiazoles 20–41, which contain differently substituted pyrrole moieties (type I compounds) (cont.).

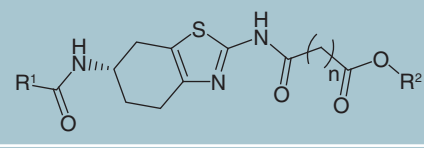

Compound	R^1	R^2	n	DNA gyrase IC_{50} [μM] or RA [%]†		Topoisomerase IV IC_{50} [μM] or RA [%]†	
				Escherichia coli	*Staphylococcus aureus*	*Escherichia coli*	*Staphylococcus aureus*
28	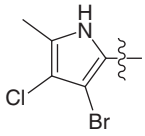	Me	1	IC_{50}: 0.25 ± 0.10	IC_{50}: 1.5 ± 0.5	RA: 74	RA: 100
29	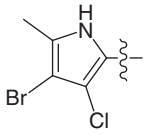	Me	1	IC_{50}: 0.056 ± 0.020	IC_{50}: 3.7 ± 1.4	RA: 91	RA: 94
30	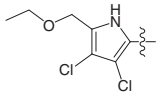	Me	1	RA: 100	n.t.	n.t.	n.t.
31[d]	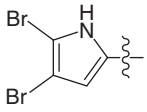	H	1	IC_{50}: 0.069 ± 0.043	IC_{50}: 86 ± 46	IC_{50}: 74 ± 30	IC_{50}: 76 ± 19
32	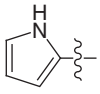	H	1	RA: 96	RA: 97	RA: 100	RA: 95
33	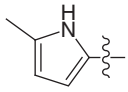	H	1	IC_{50}: 21 ± 12	RA: 94	RA: 100	RA: 99
34	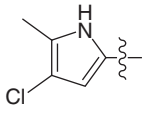	H	1	IC_{50}: 0.19 ± 0.15	IC_{50}: 2.0 ± 0.2	RA: 100	RA: 75
35	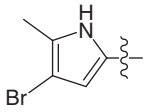	H	1	IC_{50}: 0.44 ± 0.39	IC_{50}: 7.3 ± 6.2	IC_{50}:190 ± 50	IC_{50}: 8.4 ± 4.5

†RA of the enzyme at 10 μM tested compound
‡NB was used as positive control.
¶data published previously [21].
IC_{50}: The half maximal inhibitory concentration; NB: Novobiocin; n.t.: Not tested; RA: Residual activity.

Table 1. Inhibition of *Escherichia coli* and *Staphylococcus aureus* DNA gyrase and topoisomerase IV by the 4,5,6,7-tetrahydrobenzo[*d*]thiazoles 20–41, which contain differently substituted pyrrole moieties (type I compounds) (cont.).

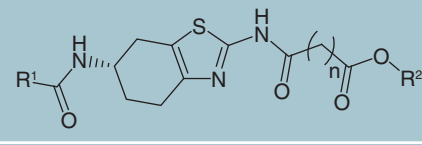

Compound	R^1	R^2	n	DNA gyrase IC_{50} [μM] or RA [%]†		Topoisomerase IV IC_{50} [μM] or RA [%]†	
				Escherichia coli	*Staphylococcus aureus*	*Escherichia coli*	*Staphylococcus aureus*
36	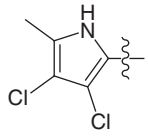	H	0	IC_{50}: 0.044 ± 0.040	IC_{50}: 0.43 ± 0.32	IC_{50}: 210 ± 20	IC_{50}: 6.2 ± 1.4
37	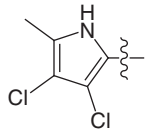	H	1	IC_{50}: 0.022 ± 0.002	IC_{50}: 0.56 ± 0.22	RA: 90	RA: 88
38	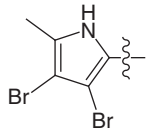	H	1	IC_{50}: 0.020 ± 0.006	IC_{50}: 12 ± 6	RA: 100	RA: 92
39	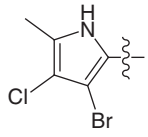	H	1	IC_{50}: 0.026 ± 0.019	IC_{50}: 0.61 ± 0.11	RA: 80	IC_{50}: 6.6 ± 2.8
40	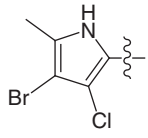	H	1	IC_{50}: 0.016 ± 0.003	IC_{50}: 1.6 ± 0.1	IC_{50}: 24 ± 15	IC_{50}: 0.73 ± 0.14
41	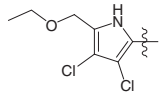	H	1	RA: 82	n.t.	RA: 100	RA: 98

†RA of the enzyme at 10 μM tested compound
‡NB was used as positive control.
¶data published previously [21].
IC_{50}: The half maximal inhibitory concentration; NB: Novobiocin; n.t.: Not tested; RA: Residual activity.

obtained from the University of Szeged (Hungary). Single-gene knock-out mutant strains of *E. coli* JW5503 (*tolC* knock-out) and JD17464 (*lpxC* knock-out) were obtained from the *E. coli* collection of the National BioResource Project at the National Institute of Genetics (Japan) [32]. *Escherichia coli* K-12 MG1655 lines carrying the clinically most commonly observed fluoroquinolone resistance mutations (GyrA S83L, D87N, D87Y; ParC S80I, E84G) and the combinations thereof were constructed in-house with the aid of the genome engineering method pORTMAGE, described in detail in previous papers [33,34]. To determine the antibacterial activities, broth microdilution assays were carried out in 96-well plates following the Clinical and Laboratory Standards Institute guidelines. For selected

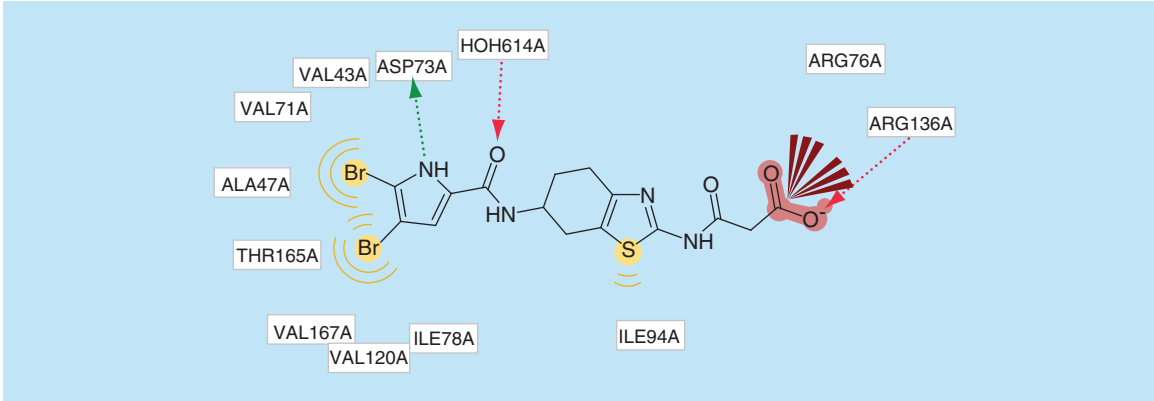

Figure 3. Interactions of representative compound I of the first generation of 4,5,6,7-tetrahydrobenzo[*d*]thiazole-based inhibitors in the *Escherichia coli* GyrB ATP-binding site, as predicted by molecular docking. Hydrophobic interactions are shown in yellow, hydrogen bonds as dashed arrows and negative charge is shown in red.

compounds, the minimum inhibitory concentrations (MICs) were determined by construction of the dose–response curves (from at least two independent experiments, each with three replicates per concentration).

Molecular modeling

Molecular docking

The crystal structure of *E. coli* DNA gyrase B in complex with adenylyl-imidodiphosphate (PDB entry: 1EI1 [35]) was used in the docking experiments, as retrieved from the Protein Data Bank. The docking calculations were carried out using the AutoDock 4.2 software [36]. In all of the calculations, the following parameters were used: the initial population of trial ligands comprised 250 individuals; the maximum number of generations was set to 270,000; the maximum number of energy evaluations was 10.0×10^6; and all of the other run parameters were maintained at their default settings. The docked conformations that resulted were clustered into families considering the backbone root mean square deviation.

Refinement of the anchoring & QTAIM analysis

After the docking calculations, the leading lowest energy structures were optimized at the M06-2X/631G(d) level using quantum mechanics/molecular mechanics calculations. The inhibitors and the side chains of the residues that had at least one heavy atom within 4 Å from the ligand molecule (i.e., first shell residues) were incorporated into the high-level QM layer using the M06-2X/631G(d) method. The chosen cut-off value resulted from a compromise between computational cost and efficiency [37,38]. The remainder of the system was included in the low-level MM layer using the Assisted Model Building with Energy Refinement (AMBER) force field. The MM parameters that were absent in the standard AMBER force field were included from the generalized AMBER force field [39]. These calculations were carried out using the Gaussian 09 package [40]. Then, the optimized geometry for each inhibitor–GyrB complex was used as the input for the quantum theory of atoms in molecules (QTAIM) analysis [41], which was carried out using the Multiwfn software [42], with the wave functions generated at the M06-2X/6-31G(d) level.

Results & discussion

Design

Novel 4,5,6,7-tetrahydrobenzo[*d*]thiazoles were designed based on the known crystal structures of inhibitors bound to the 43-kDa N-terminal fragment of *E. coli* GyrB, as described previously by our research group (PDB codes: 4ZVI, 5L3J) [23,26]. The binding site of GyrB comprises a well-defined hydrophobic pocket that consists of amino-acid residues Val43, Ala47, Val71, Ile78, Val120, and Val167 (*E. coli* GyrB numbering), and the carboxylate group of Asp73, which together with a conserved water molecule, forms a network of hydrogen bonds with the pyrrole-2-carboxamide moiety of the ligand that mimics the binding of the adenine ring of ATP [21]. Finally, additional

Table 2. Hydrogen bond strengths between the pyrrole NH and the Asp73 side-chain carboxylate group (NH ●●● O_{Asp73}) obtained from the quantum theory of atoms in molecules calculations.

Compound	$\rho_{(r)}$ NH●●●O_{Asp73}
31	0.0371
32	0.0353
33	0.0342
34	0.0352
35	0.0346
37	0.0354
38	0.0352

$\rho_{(r)}$: Atomic units (a.u.).

salt-bridge interactions with the Arg136 guanidine group and cation–π interactions between the planar aromatic ring and the Arg76 side chain within the Glu50-Arg76 salt bridge are possible in the binding site (Figure 3).

In the second generation 4,5,6,7-tetrahydrobenzo[*d*]thiazoles, we retained the pyrrole-2-carboxamide moiety to form hydrogen bonds with the binding site residues, as shown in Figure 3, while examining the steric fit of differently substituted pyrroles of varying sizes (Table 1, type **I** compounds) with the hydrophobic pocket of GyrB and ParE of *E. coli* and *S. aureus*. As the acidity of the pyrrole NH group was shown to have an important role in the binding of compounds through an influence on the strength of the hydrogen bond with the Asp73 side chain [21], we incorporated different numbers of chloro and/or bromo substituents with negative inductive effects at positions 3, 4 and 5 of the pyrrole ring. In addition, a methyl group was introduced at position 5 of the pyrrole moiety, to increase the hydrophobic interactions within the enzyme pyrrolamide binding pocket. While modifying the pyrrole moiety, the malonyl substituent on the amino group at position 2 of the 4,5,6,7-tetrahydrobenzo[*d*]thiazole core was kept constant (Figure 3) [21].

In the second stage, we fixed the pyrrolamide moiety by using either a 4,5-dibromo- or 3,4-dichloro-5-methylpyrrolamide and introduced different functionalities at position 2 of the 4,5,6,7-tetrahydrobenzo[*d*]thiazole core, which were selected to achieve additional polar interactions (i.e., hydrogen bonds and/or ionic interactions) with the positively charged side-chain guanidine groups of Arg76 and/or Arg136. The 1,3,4-oxadiazol-2-one ring was introduced as a carboxylic acid bioisostere, as it can form similar interactions with Arg136. At the same time, it is less acidic, and therefore we expected it to improve the cell-wall penetration of the compounds, and consequently their antibacterial activities [25]. Aromatic rings in compounds of the type **II** and **III** series (Tables 3 & 4) were introduced to form cation–π interactions and/or hydrogen bonds with Arg136, which would improve enzyme inhibition. In all type **I**–**III** compounds, only the (*S*)-enantiomers were prepared, as the (*R*)-enantiomers were previously shown to be weaker inhibitors of DNA gyrase than their (*S*)-antipodes [21].

Chemistry

All of the compounds were synthesized from the parent (*S*)-4,5,6,7-tetrahydrobenzo[*d*]thiazole-2,6-diamine (**9**; Figure 4), which represents the central scaffold of the designed inhibitors and was obtained according to the published procedure [43]. All of the substituted pyrroles used for the preparation of type **I** compounds were also synthesized according to the reported procedures [44]. Pyrrole-2-carboxylic acids were coupled to the 6-amino group of the central scaffold by 1-ethyl-3-(3-(dimethylamino)propyl)-carbodiimide (EDC)/1-hydroxybenzotriazole (HOBt)-promoted amide-bond formation, while the 2-trichloroacetylpyrroles were attached by heating the reaction mixtures in the presence of a base (Figure 4), to obtain compounds **10**–**19**. In the next step, acylation of the 2-amino group of **10**–**19** with methyl 3-chloro-3-oxopropanoate or ethyl 2-chloro-2-oxoacetate in the presence of triethylamine gave esters **20**–**30**, which were hydrolyzed with 1 M NaOH to the carboxylic acids **31**–**41**. Esters **20** and **26** were treated with hydrazine hydrate in dry ethanol, to obtain the hydrazides **42** and **43** (Figure 5). Compound **43** was then cyclized to the 1,3,4-oxadiazol-2-one derivative **44** (Figure 5) in the presence of 1,1′-carbonyldiimidazole (CDI).

Sulfonamides **50** and **51** were prepared as shown in Figure 6. The *tert*-butylcarbamate **45** was first reacted with methanesulfonyl chloride to obtain the sulfonamide **46**, which was then deprotected by acidolysis using HCl generated *in situ* by addition of acetyl chloride to methanol. The compound obtained, **48**, was then reacted with 2,2,2-trichloro-1-(4,5-dibromo-1*H*-pyrrol-2-yl)ethan-1-one or 3,4-dichloro-5-methyl-1*H*-pyrrole-2-carboxylic acid, to

Table 3. Inhibition of *Escherichia coli* and *Staphylococcus aureus* DNA gyrase and topoisomerase IV by the 4,5,6,7-tetrahydrobenzo[*d*]thiazole-2,6-diamine derivatives containing different moieties at 2-amino group (type II compounds).

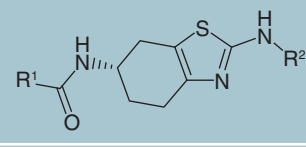

Compound	R^1	R^2	DNA gyrase IC_{50} [μM] or RA [%]†		Topoisomerase IV IC_{50} [μM] or RA [%]†	
			Escherichia coli	*Staphylococcus aureus*	*Escherichia coli*	*Staphylococcus aureus*
NB‡	-	-	IC_{50}: 0.17	IC_{50}: 0.040	IC_{50}: 11	IC_{50}: 27
42	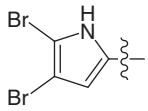	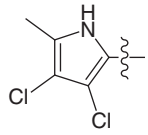	IC_{50}: 0.084 ± 0.025	RA: 73	RA: 34	RA: 95
43	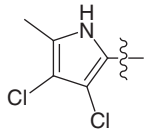	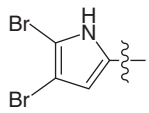	IC_{50}: 0.047 ± 0.011	IC_{50}: 0.54 ± 0.32	RA: 82	RA: 77
44	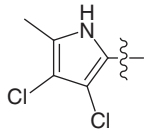	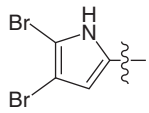	IC_{50}: 0.17 ± 0.13	RA: 33	RA: 100	RA: 93
50	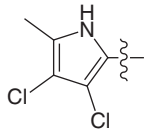	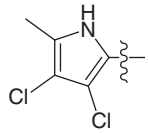	IC_{50}: 6.8 ± 0.3	n.t.	n.t.	n.t.
51	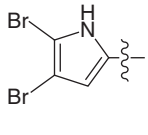	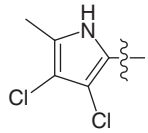	IC_{50}: 1.9 ± 0.2	RA: 75	RA: 100	RA: 100
52	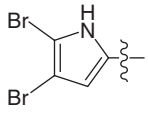	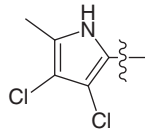	IC_{50}: 1.4 ± 0.2	n.t.	n.t.	n.t.
53	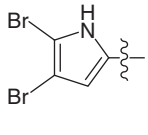	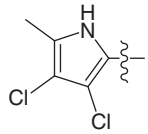	IC_{50}: 0.23 ± 0.08	RA: 74	RA: 100	RA: 99

†RA of the enzyme at 10 μM concentration of the tested compound.
‡NB was used as positive control.
IC_{50}: The half maximal inhibitory concentration; NB: Novobiocin; n.t.: Not tested; RA: Residual activity.

Table 3. Inhibition of *Escherichia coli* and *Staphylococcus aureus* DNA gyrase and topoisomerase IV by the 4,5,6,7-tetrahydrobenzo[*d*]thiazole-2,6-diamine derivatives containing different moieties at 2-amino group (type II compounds) (cont.).

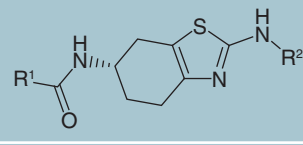

Compound	R^1	R^2	DNA gyrase IC_{50} [μM] or RA [%]†		Topoisomerase IV IC_{50} [μM] or RA [%]†	
			Escherichia coli	*Staphylococcus aureus*	*Escherichia coli*	*Staphylococcus aureus*
54	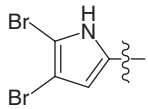	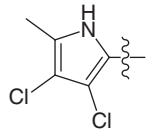	IC_{50}: 0.48 ± 0.11	RA: 71	RA: 80	RA: 100
55	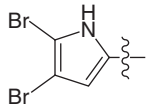	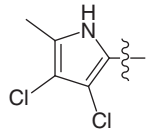	IC_{50}: 0.45 ± 0.05	RA: 87	RA: 100	RA: 100
56	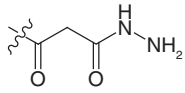	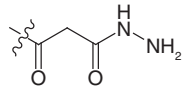	IC_{50}: 1.2 ± 0.3	RA: 66	RA: 82	RA: 100
57	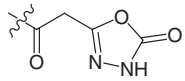		IC_{50}: 1.3 ± 0.5	n.t.	n.t.	n.t.
58		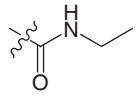	RA: 75	RA: 89	RA: 100	RA: 96
59	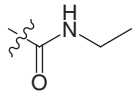		IC_{50}: 0.80 ± 0.06	n.t.	n.t.	n.t.
60	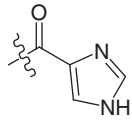	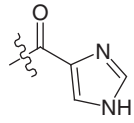	IC_{50}: 0.32 ± 0.06	RA: 91	RA: 100	RA: 100
61	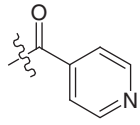	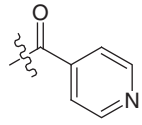	IC_{50}: 4.1 ± 0.2	RA: 100	RA: 100	RA: 97

†RA of the enzyme at 10 μM concentration of the tested compound.
‡NB was used as positive control.
IC_{50}: The half maximal inhibitory concentration; NB: Novobiocin; n.t.: Not tested; RA: Residual activity.

10.4155/fmc-2019-0127

Table 3. Inhibition of *Escherichia coli* and *Staphylococcus aureus* DNA gyrase and topoisomerase IV by the 4,5,6,7-tetrahydrobenzo[*d*]thiazole-2,6-diamine derivatives containing different moieties at 2-amino group (type II compounds) (cont.).

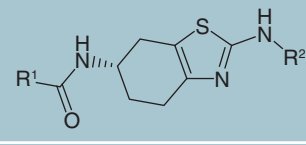

Compound	R^1	R^2	DNA gyrase IC_{50} [μM] or RA [%]†		Topoisomerase IV IC_{50} [μM] or RA [%]†	
			Escherichia coli	*Staphylococcus aureus*	*Escherichia coli*	*Staphylococcus aureus*
62	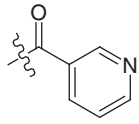	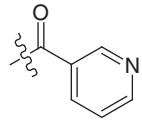	IC_{50}: 8.3 ± 0.8	n.t.	n.t.	n.t.
63	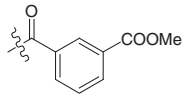	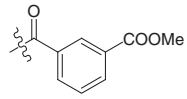	IC_{50}: 0.70 ± 0.02	RA: 94	RA: 100	RA: 99
64	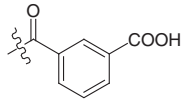	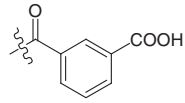	IC_{50}: 0.36 ± 0.10	n.t.	n.t.	n.t.

†RA of the enzyme at 10 μM concentration of the tested compound.
‡NB was used as positive control.
IC_{50}: The half maximal inhibitory concentration; NB: Novobiocin; n.t.: Not tested; RA: Residual activity.

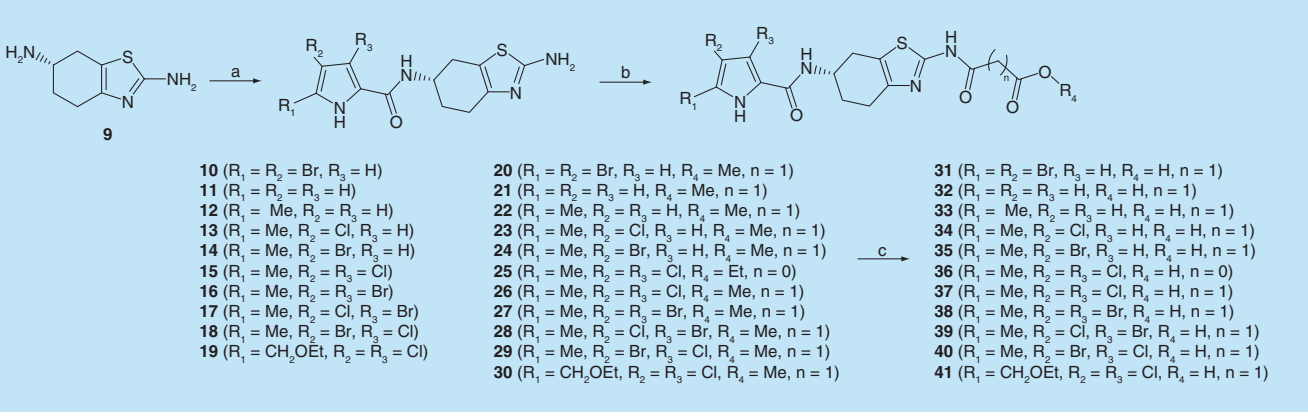

Figure 4. Reagents and conditions. (a) For **10**–**14** and **16**: corresponding 2,2,2-trichloro-1-(1*H*-pyrrol-2-yl)ethan-1-one, Na_2CO_3, N,N-dimethylformamide, 40°C, 4 h; for **15** and **17**–**19**: corresponding pyrrole-2-carboxylic acid, 1-ethyl-3-(3-(dimethylamino)propyl)-carbodiimide, 1-hydroxybenzotriazole, N-methylmorpholine, N,N-dimethylformamide, room temperature (r.t.), 18 h. (b) For **20**–**24** and **26**–**30**: methyl 3-chloro-3-oxopropanoate, Et_3N, 1,4-dioxane, r.t., 18 h; for **25**: ethyl 2-chloro-2-oxoacetate, Et_3N, 1,4-dioxane, r.t., 18 h. (c) 1 M NaOH, MeOH, room., 18 h.

yield compounds **50** and **51**, respectively. Additionally, compound **45** was treated with ethyl isocyanate, to obtain the Boc-protected ethylurea **47**. This Boc-protected ethylurea was converted to the amine **49** by acidolysis, which after coupling with 2,2,2-trichloro-1-(4,5-dibromo-1*H*-pyrrol-2-yl)ethan-1-one gave the ethylurea **52**. Alternatively, its 3,4-dichloro-5-methyl-1*H*-pyrrole-based counterpart, **53**, was prepared by reacting amine **15** with ethyl isocyanate (Figure 7). Compound **54** was prepared by acetylation of **15**, while amides **55**–**62** and **65**–**70** were prepared from **10** or **15** by EDC/HOBt or 2-(1*H*-benzotriazole-1-yl)-1,1,3,3-tetramethylaminium tetrafluoroborate

Table 4. Inhibition of *Escherichia coli* and *Staphylococcus aureus* DNA gyrase and topoisomerase IV by the 4,5,6,7-tetrahydrobenzo[*d*]thiazole-2,6-diamine derivatives containing the 2-(2-aminothiazol-4-yl)acetyl moiety at 2-amino group (type III compounds).

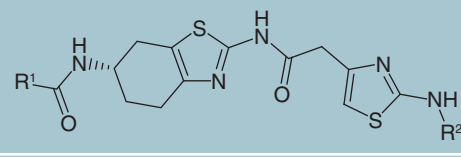

Compound	R^1	R^2	DNA gyrase IC_{50} [μM] or RA [%]†		Topoisomerase IV IC_{50} [μM] or RA [%]†	
			Escherichia coli	*Staphylococcus aureus*	*Escherichia coli*	*Staphylococcus aureus*
NB‡	-	-	IC_{50}: 0.17	IC_{50}: 0.040	IC_{50}: 11	IC_{50}: 27
65	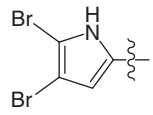	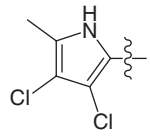	IC_{50}: 0.31 ± 0.09	RA: 64	RA: 100	RA: 99
66	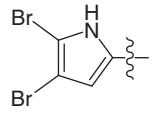	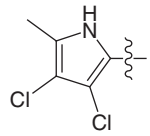	IC_{50}: 0.19 ± 0.08	n.t.	n.t.	n.t.
67	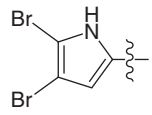	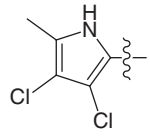	IC_{50}: 0.15 ± 0.03	RA: 23	RA: 94	RA: 96
68	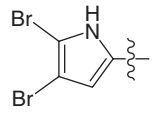		IC_{50}: 0.11 ± 0.01	RA: 67	RA: 99	RA: 100
69		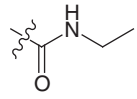	IC_{50}: 0.34 ± 0.10	RA: 100	RA: 98	RA: 99
70	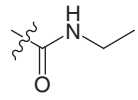	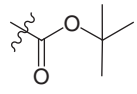	IC_{50}: 0.14 ± 0.03	RA: 76	RA: 100	RA: 99
71	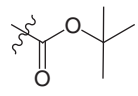	-H	IC_{50}: 2.0 ± 0.2	RA: 70	RA: 100	RA: 100

†RA of the enzyme at 10 μM concentration of the tested compound.
‡NB was used as positive control.
IC_{50}: The half maximal inhibitory concentration; NB: Novobiocin; n.t. Not tested; RA: Residual activity.

(TBTU)-promoted coupling with aromatic carboxylic acids (Figure 7). Alkaline hydrolysis of **61** and **62** gave **63** and **64**, respectively, while acidolysis of **69** yielded the amine **71** (Figure 7).

In vitro enzyme inhibition

All of these final compounds (i.e., **20**–**44**, **50**–**71**) were evaluated for their *in vitro* inhibitory activities against *E. coli* DNA gyrase using the DNA gyrase supercoiling assay. With the exception of some weekly active compounds,

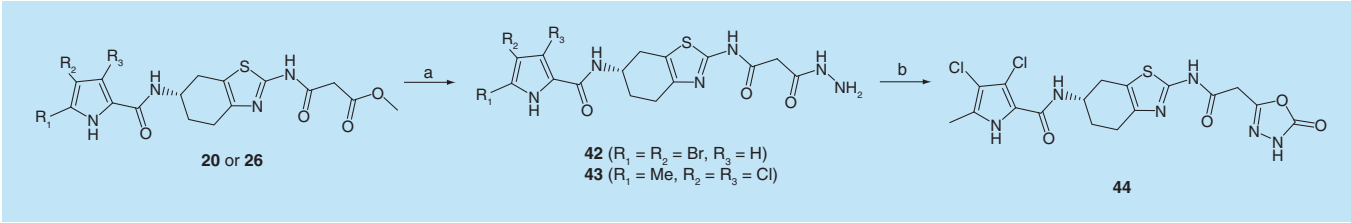

Figure 5. Reagents and conditions. (a) Hydrazine hydrate, EtOH, 80°C, 18 h. (b) 1,1′-carbonyldiimidazole, N,N-dimethylformamide, 100°C, 18 h.

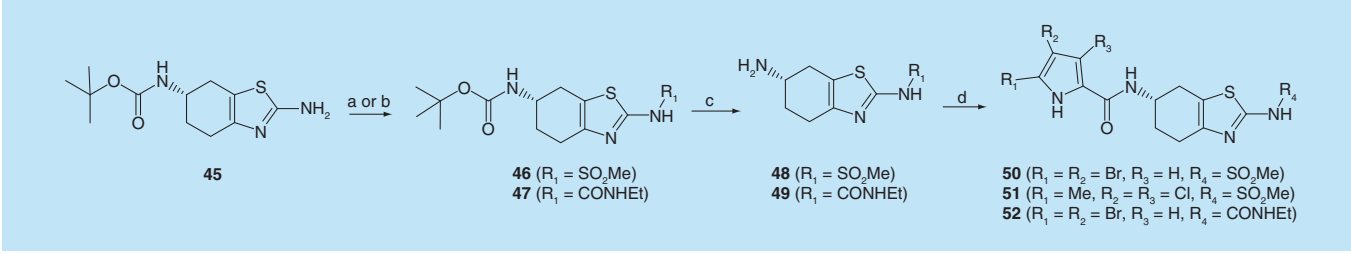

Figure 6. Reagents and conditions. (a) For **46**: methanesulfonyl chloride, pyridine, 0°C, 18 h. (b) For **47**: ethyl isocyanate, $CHCl_3$, room temperr.t.), 18 h. (c) Acetyl chloride, MeOH, 0°C, 1 h, then r.t., 18 h. (d) For **50** and **52**: 2,2,2-trichloro-1-(4,5-dibromo-1*H*-pyrrol-2-yl)ethan-1-one, Na_2CO_3, N,N-dimethylformamide, 40°C, 4 h; for **51**: 3,4-dichloro-5-methyl-1*H*-pyrrole-2-carboxylic acid, 1-ethyl-3-(3-(dimethylamino)propyl)-carbodiimide, 1-hydroxybenzotriazole, N-methylmorpholine, N,N-dimethylformamide, r.t., 18 h.

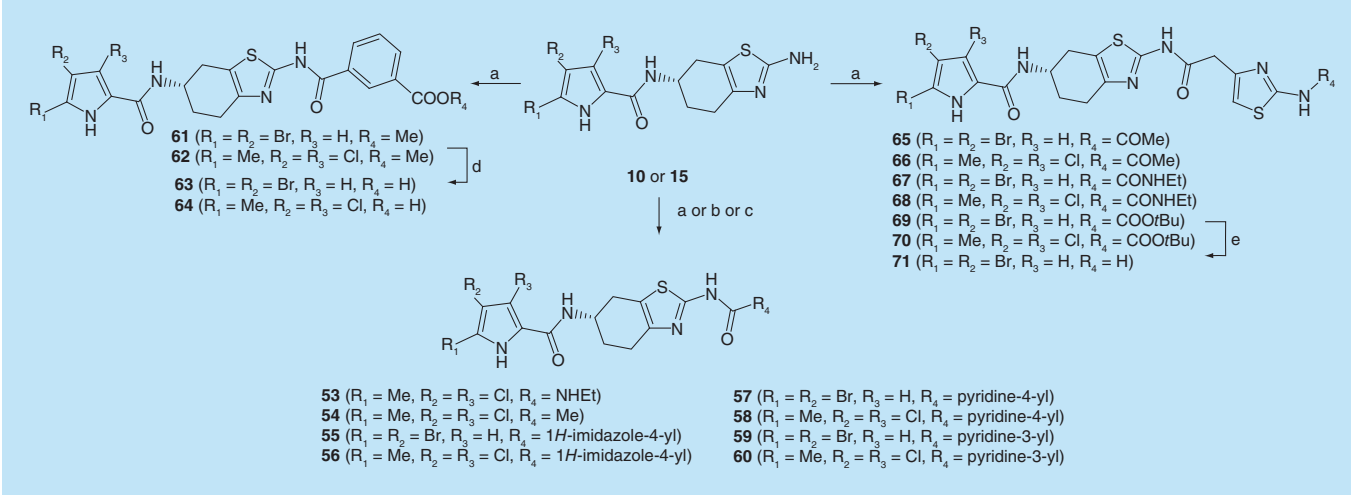

Figure 7. Reagents and conditions. (a) For **55**, **57**, **59–62**, **65–70**: carboxylic acid, 1-ethyl-3-(3-(dimethylamino)propyl)-carbodiimide, 1-hydroxybenzotriazole, N-methylmorpholine, N,N-dimethylformamide; for **56** and **58**: carboxylic acid, 2-(1H-benzotriazole-1-yl)-1,1,3,3-tetramethylaminium tetrafluoroborate, Et_3N, CH_2Cl_2, room temperature (r.t.), 24 h. (b) For **53**: ethyl isocyanate, $CHCl_3$, r.t., 18 h. (c) For **54**: acetyl chloride, Et_3N, 1,4-dioxane, r.t., 18 h. (d) 1 M NaOH, MeOH/H_2O, r.t., 24 h. (e) Acetyl chloride, MeOH, 0°C, 1 h, then r.t., 18 h.

all of these inhibitors were also tested in a DNA supercoiling assay using *S. aureus* DNA gyrase, and in a DNA relaxation assay using topoisomerase IV from *E. coli* and *S. aureus*. The results obtained are presented in Tables 1, 3, & 4 as residual activities of the enzymes at 10 μM of the tested compound, or as IC_{50} values for the more potent compounds.

Type **I** compounds (Table 1) were designed to explore the differences in the hydrophobic pockets of DNA gyrase and topoisomerase IV from *E. coli* and *S. aureus* [21], and to investigate the SARs by varying the hydrophobic character of the pyrrole moiety and the acidity of the pyrrole NH group, which was shown to interact with the

Asp73 side chain (Figure 3). In these type **I** compounds, 13 analogs showed *E. coli* DNA gyrase inhibition with IC_{50} values <0.5 μM, and with six of these <0.1 μM. These six were therefore more potent than the positive control novobiocin (IC_{50}, 0.17 μM) as well as our previously published 4,5-dibromopyrrole-based compounds **20** and **31** [21]. The most potent compound was **40**, with an IC_{50} of 0.016 μM against *E. coli* DNA gyrase, and which displayed good inhibition of all four of these enzymes, with IC_{50} values of 1.6, 24 and 0.73 μM against *S. aureus* DNA gyrase, and *E. coli* and *S. aureus* topoisomerase IV, respectively.

Extensive variations of the substituents on the pyrrole moiety revealed details of the available chemical space inside the hydrophobic pocket of all four of these investigated enzymes. Compounds **21**, **22**, **32** and **33**, containing an unsubstituted pyrrole moiety or only a methyl group on the pyrrole ring, were devoid of inhibitory activity, probably because weak hydrophobic interactions are formed in the hydrophobic pocket. On the other hand, analogs with an ethoxymethyl substituent at position 5 of the pyrrole (compounds **30** and **41**) were too bulky to fit into the pocket, and were therefore also inactive. This is in agreement with the pyrrolamide pocket volume measurements and with our previous results [21,23], where an indole moiety at this position was also unfavorable.

A combined quantum mechanics/molecular mechanics QTAIM study was performed to rationalize the observed SARs of these type **I** compounds. QTAIM calculations were performed as they enable evaluation of the molecular interactions that stabilize different ligand–enzyme complexes in detail [45–47]. We thus studied how the introduction of a methyl group and halogen atoms on the pyrrole ring influenced the strengths of interactions between the pyrrole NH and the side chain carboxylate group of Asp73 (NH ●●● O_{Asp73}). Table 2 shows the $\rho_{(r)}$ values, which represent a measure of the hydrogen bond strength, of the NH ●●● O_{Asp73} interactions for compounds **31**–**35**, **37** and **38**. The 4,5-dibromo substitution on the pyrrole ring in **31** resulted in significant increase in the strength of the NH ●●● O_{Asp73} interaction compared with the unsubstituted pyrrole in **32** (Table 2). In contrast, introduction of an electron-donating methyl group at position 5 of the pyrrole moiety in **33** weakened the NH ●●● O_{Asp73} hydrogen bond. This weakening effect of the 5-methyl group on the strength of the NH ●●● O_{Asp73} interaction can be compensated for by the introduction of halogen atoms at positions 3 and 4 of the pyrrole moiety (compounds **34**, **35**, **37**, **38**; Table 2). As the pyrrole moiety is located inside the hydrophobic pocket of the *E. coli* DNA gyrase ATP-binding site, which is formed by residues Val43, Ala47, Val71 and Val120, the methyl group and halogen atoms can form a large number of hydrophobic contacts (Supplementary Figures 1 & 2). Taken together, the cumulative effects of several hydrophobic interactions and the NH ●●● O_{Asp73} hydrogen bond strength have important effects on the *E. coli* DNA gyrase inhibition. In general, the introduction of two halogen atoms at positions 3 and 4 of the pyrrole ring improved the *E. coli* DNA gyrase inhibition due to the increased numbers of hydrophobic interactions and the increased strength of the NH ●●● O_{Asp73} hydrogen bond. The correlation obtained between the experimental IC_{50} values for **31**–**35**, **37** and **38** and $\Sigma\rho_{(r)}$ is high, as shown in Supplementary Figure 3.

For all of these type **I** compounds, acids **31**–**41** were more potent *E. coli* DNA gyrase inhibitors than their corresponding methyl or ethyl ester counterparts **20**–**30**, as they can form salt-bridge interactions with the guanidine group of the Arg136 side chain in addition to the hydrogen bond(s) formed in the case of the esters, which has also been observed previously [21,23]. The inhibitory activities against *S. aureus* DNA gyrase were weaker, which confirmed the hypothesis of the more occlusive hydrophobic pocket in *S. aureus* compared with *E. coli* GyrB [21]. The most potent inhibitors of *S. aureus* DNA gyrase were **36** and **37**, which contain the 3,4-dichloro-5-methyl-1*H*-pyrrole moiety with a smaller methyl substituent at position 5 compared with the 4,5-dibromopyrrole-containing compound **31**, which is a weak *S. aureus* DNA gyrase inhibitor (Table 1). By substitution of the chlorine atom at position 3 of the pyrrole moiety of compound **37** with a bromine atom, the inhibition of *S. aureus* DNA gyrase remained similar (compound **39**), while a bromine substituent at position 4 reduced the activity to a greater extent (compound **40**). It can thus be concluded that *S. aureus* DNA gyrase tolerates methyl or chloro substituents at positions 4 and 5 of the pyrrole ring, while larger substituents lead to a loss of inhibitory activity. Inhibition of topoisomerase IV by these type **I** compounds was weak, although on the other hand, it was improved in some cases (e.g., compound **40**, with IC_{50} values of 24 and 0.73 μM against *E. coli* and *S. aureus* topoisomerase IV, respectively) compared with the parent compound **31** (IC_{50} values of 74 and 76 μM against *E. coli* and *S. aureus* topoisomerase IV, respectively) (Table 1).

For the type **II** compounds (Table 3), the effects of the replacement of the malonyl group by different aliphatic and aromatic moieties that can form hydrogen bonds with Arg76 and/or Arg136 were investigated. In general, compounds based on 4,5-dibromopyrrole (**42**, **50, 52**, **55**, **57**, **59**, **61**, **63**) and 3,4-dichloro-5-methylpyrrole (**43**, **44**, **51**, **53**, **54**, **56**, **58**, **60**, **62**, **64**) had similar inhibitory potencies against *E. coli* DNA gyrase, but were typically

weaker inhibitors of this enzyme than most of the malonyl-based compounds in Table 1. The most potent type **II** compounds were hydrazides **42** and **43**, with *E. coli* DNA gyrase IC_{50} values of 0.084 and 0.047 μM, respectively. These two compounds showed improved inhibition in comparison with their ester counterparts **20** and **26**, but were weaker inhibitors than their corresponding carboxylic acids **31** and **37**. The hydrazide group is not ionizable under physiological conditions, and cannot form ionic interactions with the Arg136 side chain, in contrast to carboxylic acids. On the other hand, hydrazide is an H-bond donor/acceptor group and can still interact with the Arg136 guanidine group, which explains the observed inhibition potency. The introduction of aromatic rings, such as different imidazole, pyridine and substituted phenyl rings (compounds **55**–**64**), resulted in weaker inhibition of all four of these enzymes compared with the malonate derivatives of the type **I** series. All of the type **II** compounds were generally weak *E. coli* topoisomerase IV and *S. aureus* DNA gyrase and topoisomerase IV inhibitors (Table 3), which suggest that the moiety attached to the 2-amino group on the 4,5,6,7-tetrahydrobenzo[*d*]thiazole also has a very important role in the binding of compounds to the enzyme ATP-binding site. The exception is the hydrazide **43**, which was among the most potent *S. aureus* DNA gyrase inhibitors of the series, with an IC_{50} of 0.54 μM (Table 3).

The possibility of formation of cation–π interactions with the Arg136 side chain was further explored with the aminothiazole derivatives (type **III** compounds). These analogs had generally improved potencies in the *E. coli* DNA gyrase assay compared with **54**, which was without the aminothiazole moiety (Tables 3 & 4). However, the SAR data suggest that a carbonyl bound to 2-amino group of the aminothiazole moiety (compounds **65**–**70**), is important for *E. coli* DNA gyrase inhibition (IC_{50} between 0.11 and 0.34 μM), as compound **71** with a free 2-amino group was a weak inhibitor, with an IC_{50} of 2.0 μM (Table 4). All of the type **III** compounds were generally devoid of *S. aureus* DNA gyrase and topoisomerase IV and *E. coli* topoisomerase IV inhibitory activities (Table 4).

Selected compounds of types **I**-**III** were also tested for their inhibitory activities against human topoisomerase IIα, to evaluate their selectivity over the structurally and functionally similar human ATP-binding enzyme. Compounds **26**, **29**, **32**, **34**, **37**, **40** and **41** of the type **I** series and compound **60** of the type **II** series were inactive at 100 μM, which showed their selectivity for bacterial over human topoisomerases. Type **III** compounds **68** and **71** inhibited human topoisomerase IIα with residual activities of 16 and 68% at 100 μM, but were completely inactive at 10 μM.

Antibacterial activities

All of the DNA gyrase and topoisomerase IV inhibitors were tested against two Gram-positive (*E. faecalis* ATCC 29212, *S. aureus* ATCC 25923) and two Gram-negative (*E. coli* ATCC 25922, *P. aeruginosa* ATCC 27853) bacterial strains. Additionally, these compounds were tested against two *E. coli* mutant strains, as the *lpxC* deletion mutant with an impaired outer membrane (*E. coli* JD17464), and the *tolC* deletion mutant with a defective efflux pump (*E. coli* JW5503). Preliminary tests were carried out at 50 μM, and inhibition of growth was measured after 24 h of incubation. The MICs was determined only for the compounds with >90% growth inhibition at 50 μM. The results of preliminary screening are given in Supplementary Table 1, and the MICs for the active compounds are given in Table 5.

Despite potent inhibition of *E. coli* DNA gyrase by several of these compounds, and especially those from the type **I** series, they were all devoid of antibacterial activities against the tested Gram-negative wild-type *E. coli* and *P. aeruginosa* (Supplementary Table 1 & Table 5). These results can be attributed to cell-wall penetration issues of these compounds, or to their efflux, as some of them showed improved antibacterial activities against *E. coli* JW5503, which has the defective TolC efflux pump. Compound **67** was the most potent against *E. coli* JW5503, with a MIC of 3.13 μM. From the type **I** series, the esters were more potent than their acid counterparts, while for the types **II** and **III** series, the 4,5-dibromopyrrole-based compounds appeared to have better activities against *E. coli* JW5503 than their 3,4-dichloro-5-methylpyrrole-based analogs (e.g., **59** vs **60**; **67** vs **68**; see Table 5). Most of the antibacterially active compounds are potent *E. coli* DNA gyrase inhibitors that are lipophilic and do not contain ionizable groups.

In general, the antibacterial activities of these tested compounds were better against Gram-positive *S. aureus* and *E. faecalis* than against Gram-negative *E. coli* and *P. aeruginosa* (Supplementary Table 1 & Table 5). The most potent compound against *S. aureus* was **27**, with a MIC of 25 μM, while for *E. faecalis*, **29** had the lowest MIC of the series, at 12.5 μM (Table 5). Both of these compounds are methyl esters, which were weaker inhibitors of DNA gyrase than their carboxylic acid counterparts **38** and **40**, respectively. This might be explained by the excessive

Table 5. Minimum inhibitory concentrations of the DNA gyrase and topoisomerase IV inhibitors.

Compound	MIC [μM]†					
	Enterococcus faecalis	*Staphylococcus aureus*	*Escherichia coli*			*P. aeruginosa*
	ATCC 29212	ATCC 25923	ATCC 25922	JW5503	JD17464	ATCC 27853
24	>50	>50	>50	50 (23)	>50	>50
26	50 (22)	50 (22)	>50	12.5 (6)	>50	>50
27	25 (13)	25 (13)	>50	12.5 (7)	>50	>50
28	>50	>50	>50	12.5 (6)	>50	>50
29	12.5 (6)	>50	>50	12.5 (6)	>50	>50
42	>50	>50‡	>50	25 (13)	>50	>50
43	>50	>50	>50	25 (11)	>50	>50
44	50 (24)	50 (24)	>50	25 (12)	>50	>50
52	>50	>50	>50	12.5 (6)	>50	>50
55	>50	>50	>50	6.25 (3)	>50	>50
59	>50	>50	>50	12.5 (7)	>50	>50
65	>50	>50	>50	6.25 (4)	>50	>50
67	>50	>50	>50	3.13 (2)	>50	>50
68	50 (28)	>50‡	>50	>50	>50	>50
Ciprofloxacin	3.0	1.5	0.05	0.015	0.12	3.0

†MIC: Minimum inhibitory concentration that inhibits the growth of bacteria by ≥90%. Values in parentheses are MIC values expressed in μg/ml.
‡Tested against *Staphylococcus aureus* ATCC 29213.
MIC: Minimum inhibitory concentration.

Table 6. Antibacterial activities of 24, 27, and 29 against additional Gram-positive bacterial strains.

Compound	MIC [μg/ml]			
	Staphylococcus aureus			*Enterococcus faecium*
	ATCC 29213	ATCC 43300 (MRSA)	ATCC 700699 (VISA)	ATCC 700221
24	64	64	32	64
27	8	16	8	16
29	8	8	4	8

Values in parentheses are MIC values expressed in μg/ml.
MIC: Minimum inhibitory concentration that inhibits the growth of bacteria by ≥90%; MRSA: Methicillin-resistant *Staphylococcus aureus*; VISA: Vancomycin-intermediate *Staphylococcus aureus*.

polarity and acidity of the carboxylic acids (Table 1); they therefore cannot permeate through the bacterial cell wall, which results in low on-target concentrations of these inhibitors. In addition, compounds **24**, **27** and **29** showed promising activities also against methicillin-resistant *S. aureus*, vancomycin-intermediate *S. aureus* and *E. faecium*, with MICs between 4 and 16 μg/ml (Table 6). Moreover, compounds **27** and **29** displayed no cross-resistance with fluoroquinolones as they showed improved MIC values against fluoroquinolone-resistant strains of *E. coli* compared with the wild-type (Table 7). In conclusion here, the correlation between DNA gyrase/topoisomerase IV inhibition and antibacterial activity against Gram-positive and Gram-negative strains was weak, as has been reported previously [10,48].

Conclusion

Three series of structural analogs of 4,5,6,7-tetrahydrobenzo[*d*]thiazole-based DNA gyrase B inhibitors were designed, synthesized and biologically evaluated. The results of the *in vitro E. coli* and *S. aureus* DNA gyrase and topoisomerase IV inhibition assays showed improved activities of some of the type **I** compounds against all four enzymes, when compared with our previously reported series [21]. The type **II** and **III** compounds showed nanomolar *E. coli* DNA gyrase inhibition, but were generally weak *S. aureus* DNA gyrase and *E. coli* and *S. aureus* topoisomerase IV inhibitors. Importantly, the improved enzyme inhibition of the type **I** compounds also resulted in antibacterial activities against some Gram-positive strains, which was not seen for in the previously reported series of 4,5,6,7-tetrahydrobenzo[*d*]thiazoles [21]. Compound **29** inhibited *E. coli* and *S. aureus* DNA gyrase with

Table 7. Antibacterial activities of **27** and **29** against fluoroquinolone-resistant *Escherichia coli*.

Compound	MIC [μg/ml]†				
	Escherichia coli K-12 MG1655				
	Wild type	GyrA S83L	GyrA S83L, D87N	GyrA S83L, D87Y; ParC S80I	GyrA S83L, D87N; ParC S80I, E84G
Ciprofloxacin	0.5	0.156	0.313	12.5	50
27	>50	25	6.25	25	25
29	>50	25	12.5	25	25

†Tested in the presence of efflux pump inhibitor phenylalanine-arginine β-naphthylamide (PAβN; 50 μg/ml).
Values in parentheses are MIC values expressed in μg/ml.
MIC: Minimum inhibitory concentration that inhibits the growth of bacteria by ≥90%.

IC_{50} values of 0.056 and 3.7 μM, respectively, and showed activity against *S. aureus*, methicillin-resistant *S. aureus*, vancomycin-intermediate *S. aureus*, and *E. faecium*, with MICs between 4 and 16 μg/ml. Compound **29** thus represents a good starting point for further optimization.

Future perspective

The emerging field of multidrug resistance among bacteria calls for urgent need to develop novel effective antibiotics with alternative mechanisms of action, which would more likely not be as susceptible to the pre-existing resistance mechanisms. A lot of efforts have been made in the last decades to identify novel ATPase inhibitors of DNA gyrase and topoisomerase IV. Especially in the last few years, some of them have reached clinical trials [11], which again awakened optimism in these new-class antibacterials after novobiocin was withdrawn from the market in 2011. However, none of these compounds has so far been approved for therapeutic use. For sure, economical reasons hinder the development of novel antibacterials, because newly discovered antibiotics are usually held in reserve and prescribed only after the available treatment options have been exhausted. Meanwhile, in the case of first-in-class antibacterial agents the situation is better and the initial investment often pays off, such as in the case of linezolid and daptomycin [10]. One of the possible strategies for improving antibacterial activities of the presented 4,5,6,7-tetrahydrobenzo[*d*]thiazole class of GyrB inhibitors would be to make compounds less acidic in order to improve penetration through the bacterial cell wall. In addition, enzyme inhibition should be improved further by strengthening the salt bridge formation with Arg136 and/or cation–π interaction with Arg76 (*E. coli* numbering). The substantial amount of accumulated knowledge in the field of DNA gyrase and topoisomerase IV inhibitors offers opportunity to approach the development of these inhibitors with greater confidence in the future. Thus, clinically approved drugs from this class are hopefully not far away.

Summary points

- DNA gyrase and topoisomerase IV are important targets for designing novel antibacterials to overcome bacterial resistance problems.
- Starting from our previous series of the 4,5,6,7-tetrahydrobenzo[*d*]thiazole-based DNA gyrase B inhibitors, a structure–activity relationship of these compounds was further explored and up-graded.
- Newly prepared analogs showed nanomolar enzyme inhibition of DNA gyrase and topoisomerase IV and the most potent was **40**, with an IC_{50} of 0.016 μM against *Escherichia coli* DNA gyrase.
- Compounds also showed improved *in vitro* antibacterial activity against Gram-positive strains and analog **29** possessed activity against methicillin-resistant *Staphylococcus aureus* and Vancomycin-intermediate *Staphylococcus aureus* with minimum inhibitory concentrations between 4 and 8 μg/ml, thus representing a promising hit for further optimization studies.

Supplementary data

To view the supplementary data that accompany this paper please visit the journal website at: www.future-science.com/doi/suppl/10.4155/fmc-2019-0127

Acknowledgments

The authors thank D Žigon (Mass Spectrometry Centre, Jožef Stefan Institute, Ljubljana, Slovenia) for the mass spectra, Heidi Mäkkylä, Cristina Carbonell Duacastella and H Parviainen for their technical assistance in the antibacterial assays and C Berrie for scientific editing of the manuscript.

Financial & competing interests disclosure

The work was funded by the Slovenian Research Agency (grant no. P1-0208, Bilateral project Slovenia – Argentina BI-AR/2018-2019-004), Academy of Finland (grant no. 277001, 304697, 312503), the European Research Council H2020-ERC-2014-CoG 648364 – Resistance Evolution (to C Pál), the Wellcome Trust (to C Pál), and GINOP (MolMedEx TUMORDNS) GINOP-2.3.2-15-2016-00020 and GINOP (EVOMER) GINOP-2.3.2-15-2016-00014 (to C Pál), the 'Lendület' Programme of the Hungarian Academy of Sciences (to C Pál), and a PhD Fellowship from the Boehringer Ingelheim Fonds (to Á Nyerges). The authors have no other relevant affiliations or financial involvement with any organization or entity with a financial interest in or financial conflict with the subject matter or materials discussed in the manuscript apart from those disclosed.

No writing assistance was utilized in the production of this manuscript.

References

Papers of special note have been highlighted as: • of interest; •• of considerable interest

1. Santajit S, Indrawattana N. Mechanisms of antimicrobial resistance in ESKAPE pathogens. *Biomed. Res. Int.* 2016, 2475067 (2016).
2. World Health Organization. WHO publishes list of bacteria for which new antibiotics are urgently needed (2017). www.who.int/news-room/detail/27-02-2017-who-publishes-list-of-bacteria-for-which-new-antibiotics-are-urgently-needed
3. Fernandes P, Martens E. Antibiotics in late clinical development. *Biochem. Pharmacol.* 133, 152–163 (2017).
4. Gonzalez-Bello C. Antibiotic adjuvants – a strategy to unlock bacterial resistance to antibiotics. *Bioorg. Med. Chem. Lett.* 27(18), 4221–4228 (2017).
5. Tse-Dinh YC. Targeting bacterial topoisomerases: how to counter mechanisms of resistance. *Future Med. Chem.* 8(10), 1085–1100 (2016).
6. Sissi C, Palumbo M. In front of and behind the replication fork: bacterial type IIA topoisomerases. *Cell. Mol. Life Sci.* 67(12), 2001–2024 (2010).
7. Collin F, Karkare S, Maxwell A. Exploiting bacterial DNA gyrase as a drug target: current state and perspectives. *Appl. Microbiol. Biotechnol.* 92(3), 479–497 (2011).
8. Chopra S, Matsuyama K, Tran T *et al.* Evaluation of gyrase B as a drug target in *Mycobacterium tuberculosis*. *J. Antimicrob. Chemother.* 67(2), 415–421 (2012).
9. Tomašič T, Peterlin Mašič L. Prospects for developing new antibacterials targeting bacterial type IIA topoisomerases. *Curr. Top. Med. Chem.* 14(1), 130–151 (2014).
10. Bisacchi GS, Manchester JI. A new-class antibacterial – almost. Lessons in drug discovery and development: a critical analysis of more than 50 years of effort toward ATPase inhibitors of DNA gyrase and topoisomerase IV. *ACS Infect. Dis.* 1(1), 4–41 (2015).

•• **An exhaustive and detailed overview of development of DNA gyrase and topoisomerase IV inhibitors as well as critical analysis of research efforts in this field since 1960s.**

11. Durcik M, Tomašič T, Zidar N *et al.* ATP-competitive DNA gyrase and topoisomerase IV inhibitors as antibacterial agents. *Expert Opin. Ther. Pat.* 29(3), 171–180 (2019).

• **Recent review on development of ATP-competitive DNA gyrase and topoisomerase IV inhibitors in the last 10 years.**

12. Anderson VE, Osheroff N. Type II topoisomerases as targets for quinolone antibacterials: turning Dr. *Jekyll into Mr. Hyde*. *Curr. Pharm. Des.* 7(5), 337–353 (2001).
13. Drlica K, Malik M, Kerns RJ, Zhao X. Quinolone-mediated bacterial death. *Antimicrob. Agents Chemother.* 52(2), 385–392 (2008).
14. Sanyal G, Doig P. Bacterial DNA replication enzymes as targets for antibacterial drug discovery. *Expert Opin. Drug Discov.* 7(4), 327–339 (2012).
15. Taylor SN, Morris DH, Avery AK *et al.* Gepotidacin for the treatment of uncomplicated urogenital gonorrhea: a Phase II, randomized, dose-ranging, single-oral dose evaluation. *Clin. Infect. Dis.* 67(4), 504–512 (2018).
16. De Ambrogi M, McConnell J, Mushtaq A. Highlights from the 26th ECCMID. *Lancet Infect. Dis.* 16(6), 645–647 (2016).
17. Hameed PS, Solapure S, Mukherjee K *et al.* Optimization of pyrrolamides as mycobacterial GyrB ATPase inhibitors: structure–activity relationship and *in vivo* efficacy in a mouse model of tuberculosis. *Antimicrob. Agents Chemother.* 58(8), 4993–4994 (2014).
18. Škedelj V, Tomašič T, Mašič LP, Zega A. ATP-binding site of bacterial enzymes as a target for antibacterial drug design. *J. Med. Chem.* 54(4), 915–929 (2011).

19. Tari LW, Li X, Trzoss M *et al.* Tricyclic GyrB/ParE (TriBE) inhibitors: a new class of broad-spectrum dual-targeting antibacterial agents. *PLoS ONE* 8(12), e84409 (2013).
20. Aldred KJ, Kerns RJ, Osheroff N. Mechanism of quinolone action and resistance. *Biochemistry* 53(10), 1565–1574 (2014).
21. Tomašič T, Katsamakas S, Hodnik Ž *et al.* Discovery of 4,5,6,7-tetrahydrobenzo[1,2-*d*]thiazoles as novel DNA gyrase inhibitors targeting the ATP-binding site. *J. Med. Chem.* 58(14), 5501–5521 (2015).

- **Describes the first generation of 4,5,6,7-tetrahydrobenzo[*d*]thiazole-based DNA gyrase inhibitors and initial structure–activity relationship studies.**

22. Zidar N, Tomašič T, Macut H *et al.* New *N*-phenyl-4,5-dibromopyrrolamides and *N*-phenylindolamides as ATPase inhibitors of DNA gyrase. *Eur. J. Med. Chem.* 117, 197–211 (2016).
23. Zidar N, Macut H, Tomašič T *et al. N*-Phenyl-4,5-dibromopyrrolamides and *N*-phenylindolamides as ATP competitive DNA gyrase B inhibitors: design, synthesis, and evaluation. *J. Med. Chem.* 58(15), 6179–6194 (2015).
24. Durcik M, Lovison D, Skok Ž *et al.* New *N*-phenylpyrrolamide DNA gyrase B inhibitors: optimization of efficacy and antibacterial activity. *Eur. J. Med. Chem.* 154, 117–132 (2018).
25. Durcik M, Tammela P, Barančoková M *et al.* Synthesis and evaluation of *N*-phenylpyrrolamides as DNA gyrase B inhibitors. *ChemMedChem* 13(2), 186–198 (2018).
26. Gjorgjieva M, Tomašič T, Barančoková M *et al.* Discovery of benzothiazole scaffold-based DNA gyrase B inhibitors. *J. Med. Chem.* 59(19), 8941–8954 (2016).

- **Additional structure–activity relationship studies on benzothiazole-2,6-diamine scaffold with x-ray structure of DNA gyrase B in complex with inhibitor.**

27. Tomašič T, Mirt M, Barančoková M *et al.* Design, synthesis and biological evaluation of 4,5-dibromo-*N*-(thiazol-2-yl)-1*H*-pyrrole-2-carboxamide derivatives as novel DNA gyrase inhibitors. *Bioorg. Med. Chem.* 25(1), 338–349 (2017).

- **A series of »reversed« and ring-opened DNA gyrase inhibitors based on the 4,5,6,7-tetrahydrobenzo[*d*]thiazole scaffold.**

28. Flatman RH, Eustaquio A, Li SM, Heide L, Maxwell A. Structure–activity relationships of aminocoumarin-type gyrase and topoisomerase IV inhibitors obtained by combinatorial biosynthesis. *Antimicrob. Agents Chemother.* 50(4), 1136–1142 (2006).
29. Phillips JW, Goetz MA, Smith SK *et al.* Discovery of Kibdelomycin, A potent new class of bacterial type II topoisomerase inhibitor by chemical-genetic profiling in *Staphylococcus aureus. Chem*. *Biology* 18(8), 955–965 (2011).
30. Basarab GS, Hill PJ, Garner CE *et al.* Optimization of pyrrolamide topoisomerase II inhibitors toward identification of an antibacterial clinical candidate (AZD5099). *J. Med. Chem.* 57(14), 6060–6082 (2014).
31. Yule IA, Czaplewski LG, Pommier S, Davies DT, Narramore SK, Fishwick CWG. Pyridine-3-carboxamide-6-yl-ureas as novel inhibitors of bacterial DNA gyrase: structure based design, synthesis, SAR and antimicrobial activity. *Eur. J. Med. Chem.* 86, 31–38 (2014).
32. Baba T, Ara T, Hasegawa M *et al.* Construction of *Escherichia coli* K-12 in-frame, single-gene knockout mutants: the Keio collection. *Mol. Syst. Biol.* 2, 2006.0008 (2006).
33. Nyerges Á, Csörgő B, Nagy I *et al.* A highly precise and portable genome engineering method allows comparison of mutational effects across bacterial species. *Proc. Natl Acad. Sci. USA* 113, 2502–2507 (2016).
34. Nyerges Á, Csörgő B, Draskovits G *et al.* Directed evolution of multiple genomic loci allows the prediction of antibiotic resistance. *Proc. Natl Acad. Sci. USA* 115, E5726–E5735 (2018).
35. Brino L, Urzhumtsev A, Mousli M *et al.* Dimerization of *Escherichia coli* DNA-gyrase B provides a structural mechanism for activating the ATPase catalytic center. *J. Biol. Chem.* 275(13), 9468–9475 (2000).
36. Morris GM, Huey R, Lindstrom W *et al.* AutoDock4 and AutoDockTools4: automated docking with selective receptor flexibility. *J. Comput. Chem.* 30(16), 2785–2791 (2009).
37. Guo XC, He DY, Huang L, Liu LM, Liu LJ, Yang HJ. Strain energy in enzyme-substrate binding: an energetic insight into the flexibility versus rigidity of enzyme active site. *Comput. Theor. Chem.* 995, 17–23 (2012).
38. Guo XC, He DY, Liu LM, Kuang RY, Liu LJ. Use of QM/MM scheme to reproduce macromolecule-small molecule noncovalent binding energy. *Comput. Theor. Chem.* 991, 134–140 (2012).
39. Wang JM, Wolf RM, Caldwell JW, Kollman PA, Case DA. Development and testing of a general amber force field. *J. Comput. Chem.* 25(9), 1157–1174 (2004).
40. Frisch MJ, Trucks GW, Schlegel HB *et al.* Gaussian 09, Revision A.02, Gaussian, Inc., CT, USA (2016).
41. Bader RFW. Atoms in molecules. *Acc. Chem. Res.* 18(1), 9–15 (1985).
42. Lu T, Chen FW. Multiwfn: a multifunctional wavefunction analyzer. *J. Comput. Chem.* 33(5), 580–592 (2012).
43. Schneider CS, Mierau J. Dopamine autoreceptor agonists – resolution and pharmacological activity of 2,6-diaminotetrahydrobenzothiazole and an aminothiazole analog of apomorphine. *J. Med. Chem.* 30(3), 494–498 (1987).
44. Breeze AL, Green OM, Hull KG *et al.* Pyrrol derivatives with antibacterial activity. WO 2005/026149 A1 (2005).

45. Vettorazzi M, Menendez C, Gutierrez L, Andujar S, Appignanesi G, Enriz RD. Theoretical models to predict the inhibitory effect of ligands of sphingosine kinase 1 using QTAIM calculations and hydrogen bond dynamic propensity analysis. *J. Comput. Aided Mol. Des.* 32(7), 781–791 (2018).

46. Tosso RD, Andujar SA, Gutierrez L *et al.* Molecular modeling study of dihydrofolate reductase inhibitors. Molecular dynamics simulations, quantum mechanical calculations, and experimental corroboration. *J. Chem. Inf. Model.* 53(8), 2018–2032 (2013).

47. Andujar SA, Tosso RD, Suvire FD *et al.* Searching the "biologically relevant" conformation of dopamine: a computational approach. *J. Chem. Inf. Model.* 52(1), 99–112 (2012).

48. Manchester JI, Dussault DD, Rose JA *et al.* Discovery of a novel azaindole class of antibacterial agents targeting the ATPase domains of DNA gyrase and topoisomerase IV. *Bioorg. Med. Chem. Lett.* 22(15), 5150–5156 (2012).